ON THE FOLDS AND FRACTURE CLEAVAGES IN THE NIMBAHERA LIMESTONES AT CHITORGARH, RAJASTHAN

by A. K. Saha *and* P. K. Gangopadhyay, *Department of Geology, Presidency College, Calcutta*

(Communicated by S. Deb, F.N.I.)

(*Received December 20, 1963; after revision April 25, 1964*)

The Nimbahera limestone forming part of the late pre-Cambrian Vindhyan System occurs just west of the Chitorgarh Fort in Rajasthan. The structures in a well-exposed part of the limestone measuring about 900 m by 350 m have been mapped on a scale of 1 : 1,200 and studied. The limestones show a major anticline slightly overturned to the east and plunging 7°–22° towards N 10° W–N 20° W. The eastern limb of the major anticline discloses four pairs of related subsidiary anticlines and synclines. Three of these die out within the southern limit of the mapped area. The folding of the limestone band is conical on a large scale and cylindrical in small segments. The limestone displays two sets of discrete, close-spaced intersecting fracture cleavages (S_2 and S_3) with distinct fanning of both the sets around the folds. It is shown that the Nimbahera limestone was folded on NNW axes by flexural slip. Fracture cleavage S_2 developed parallel to the axial planes of folds at an initial stage of folding. With continuation of folding S_2 became passive as the stress pattern changed slightly and another set of fracture cleavage, S_3, developed parallel to the prevailing axial planes of folds; locally pronounced slip on S_3 helped extension of the rock mass in a sub-vertical direction—a fact corroborated by petrofabric study of orientation of optic axes of elongated calcite crystals in the limestones. A set of transverse joints, a set of minor, widely spaced fractures (S_4) and some zones of 'drag' formed during the late stage of deformation.

1. Introduction

Just west of Chitorgarh Fort in Rajasthan occurs a 120 m to 150 m thick band of limestone, called the Nimbahera limestone, forming part of the late pre-Cambrian Vindhyan System (Heron 1936). This unmetamorphosed limestone band, together with the shales and slaty shales above and below, is folded into a system of narrow, open, gently plunging anticlines and synclines trending nearly north-south (Fig. 1, inset). In the autumn of 1962, the authors had an occasion to examine the structural features displayed by these limestones which provide excellent materials for the study of (i) the relationship between fracture cleavage and folding and (ii) the mechanics of folding and formation of fracture cleavages in these rocks. They carried out a systematic detailed study (including mapping on a scale 1 : 1,200) of the structures in a small but excellently exposed area of the limestones measuring about 900 m

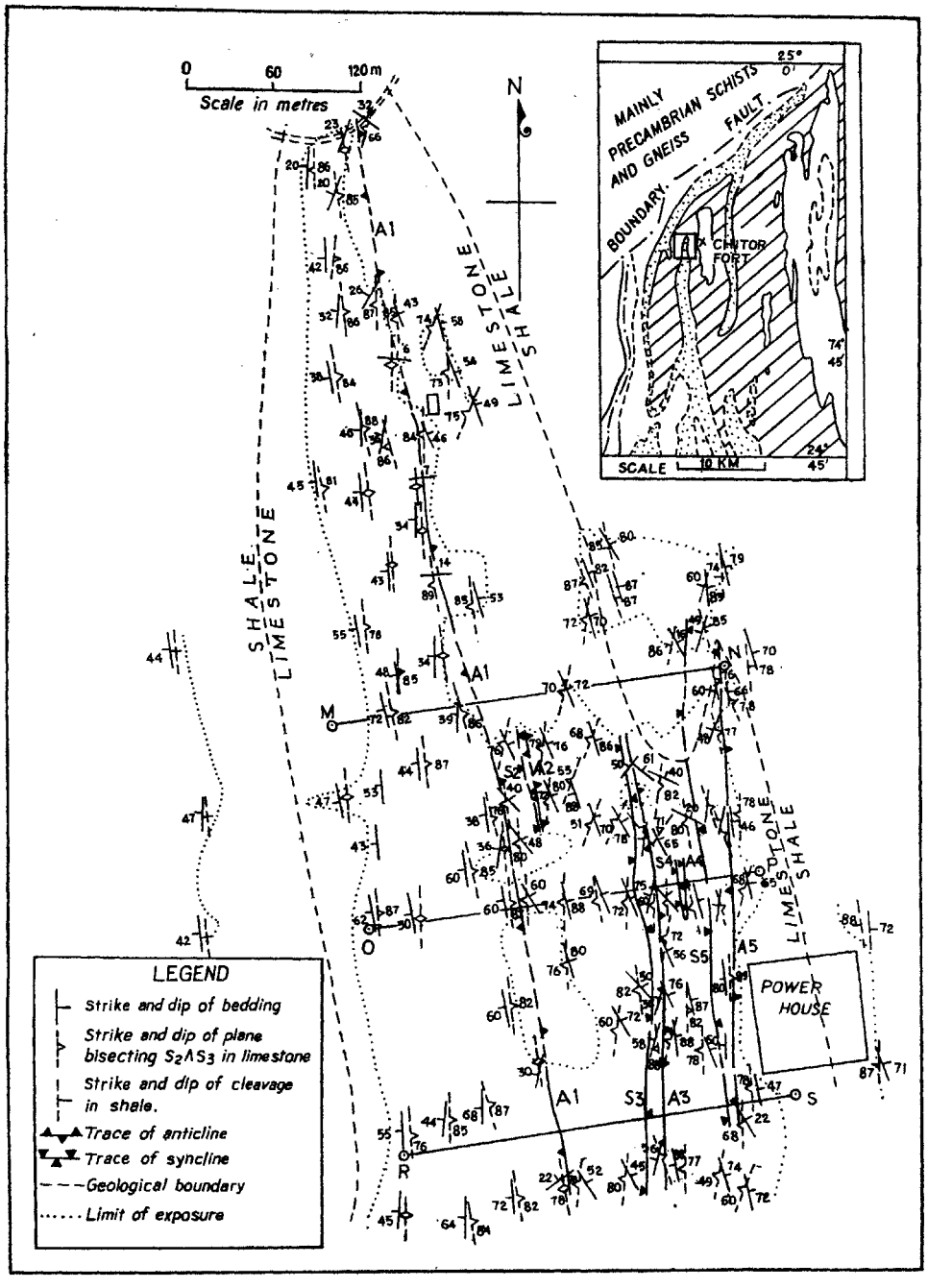

FIG. 1. Structural map of the area near the Power House, just west of the Chitorgarh Fort, Rajasthan. Inset map (after Heron 1936, plate 22) shows the location of the area together with the regional geology of Chitorgarh. Vindhyan rocks lie south-east of Boundary Fault with Nimbahera limestone shown in stipples and Suket shales in stripes; other rock units unornamented.

by 350 m, just west of Chitorgarh Fort and north of the newly built Power House (Fig. 1). The present paper deals primarily with the structures of this interesting, though small, area.

Previous work.—The limestone area under consideration forms a part of the large region of SE Rajputana mapped geologically by Heron (1936), who referred to the folds and the resulting 'vague cleavage' in the Nimbahera limestone. He did not, however, measure the 'cleavage', nor did he study its spatial relationship with folding (Heron 1936, p. 79). Details of stratigraphy and lithology of Chitorgarh area have been given by Heron (1936).

2. Description of the Structures

General.—The Nimbahera limestone of Chitorgarh is generally light grey to dark bluish grey, fine-grained and well-bedded; the individual layers are usually 30 cm or less in thickness, and they alternate with thin (less than 1 cm thick) argillaceous or siliceous layers. Within the individual layers again, there are very thin laminations of various colours. The Nimbahera shales lying below the limestone are purple to grey, finely laminated slaty shales; they pass up into the limestones through a zone of purple, slabby, silty shale. The Suket shales, which overlie the limestones, are bluish grey to purple very finely laminated slaty rocks; a set of closely spaced fracture cleavage intersects the lamination, usually at high angles.

Folds.—The limestones in the flat, slightly undulating area near the Power House (Fig. 1) show a major anticline (A.1), plunging at 7°–22° towards N 10° W–N 20° W. This fold is slightly overturned to the east, the average axial plane dipping at 88° towards S 86° W (cf. Figs. 2, 3 and 4). The eastern limb of the major anticline shows four pairs of synclines and anticlines (S.2–A.2; S.3–A.3; S.4–A.4; S.5–A.5) whose axial traces are sub-parallel to that of the major anticline. All these folds are characteristically narrow and have fairly sharp, though round, hinges.

The subsidiary folds are much less persistent than the main fold, the S.2–A.2 and S.4–A.4 pairs being traceable for only about 70 m and 40 m respectively. The other two sets of folds are more persistent, the S.5–A.5 pair being traceable for about 350 m, while the S.3–A.3 pair has been traced for about 300 m and it continues further south of the area mapped.

As in the major anticline, the subsidiary anticline-syncline pairs have steep west-dipping axial planes and low northerly plunges (Table I).

The values of the fold plunges given in Table I, except that for the fold pair S.4–A.4, are based on the maximum concentrations of the intersections of the bedding planes within approximately 8 m on either side of the respective axial traces (Figs. 2–7).

The maxima agree well with the direct measurements of the plunge on the hinges of the respective folds. The subsidiary folds thus have, in general,

TABLE I

Attitudes of the folds, Chitorgarh Power House area

Fold No.	Average plunge of hinge	Dip of axial plane
A.1 (north) ..	11°/N 15° W	84°/S 76° W
A.1 (centre) ..	12°/N 14° W	86°/S 78° W
A.1 (south) ..	20°/N 15° W	78°/S 80° W
S.2–A.2 ..	20°/N 17° W	84°/S 75° W
S.3–A.3 ..	22°/N 15° W	72°/W
S.4–A.4 ..	26°/N 6° W	88°/S 85° W
S.5–A.5 ..	15°/N 8° W	86°/S 87°W

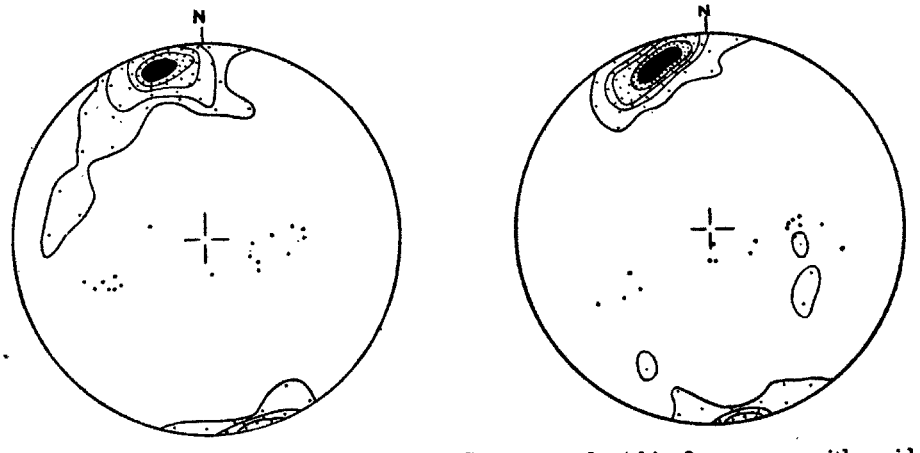

FIG. 2. β-diagram of the bedding planes (S_1) measured within 8 metres on either side of the main anticline, A.1 (northern part). 153 β-intersections. Contours at 30-20-10-5-1 per cent per 1 per cent area. Dots stand for πS_1-poles.

FIG. 3. β-diagram of the bedding planes (S_1) measured within 8 metres on either side of the main anticline, A.1 (central part). 136 β-intersections. Contours at 30-20-10-5-1 per cent per 1 per cent area. Dots stand for πS_1-poles.

steeper plunges than the main anticline; also the plunges of all the folds are generally steeper towards the south.

The axial traces of the subsidiary folds on the eastern limb of the main anticline indicate a slight but distinct radial arrangement, these folds being closer together in the south than in the north. On a small scale, this tendency is suggested by the folds S.4 and A.4 which ultimately coalesce and die out towards south.

The eastern limb of the main anticline is locally vertical and even overturned in between A.2 and S.3, where westerly dips of 82°–85° are found locally.

The western limb of the main anticline is free from the complexities of the subsidiary folds. Of special interest here are some local small-scale contortions of the bedding plane on moderately steep (40°–60°) north-westerly plunging axes. Also two monoclinal 'rolls' (individual 'rolls' traceable for about 10 m) with axes parallel to that of the main anticline have been noted;

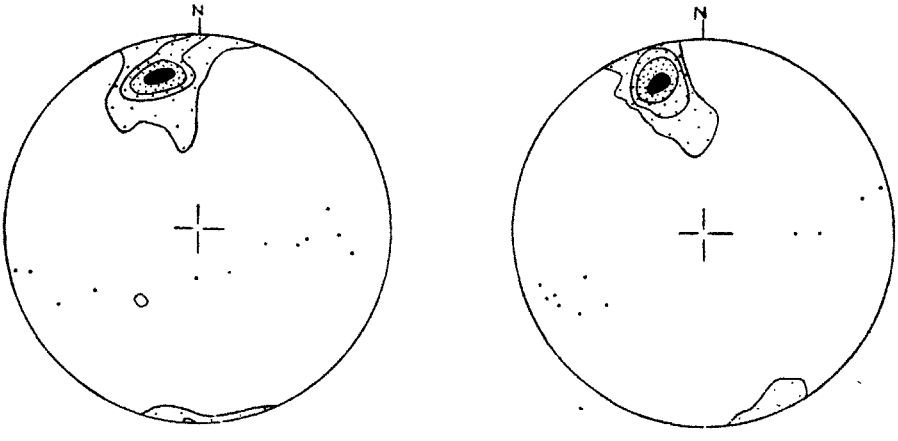

FIG. 4. β-diagram of the bedding planes (S_1) measured within 8 metres on either side of the main anticline, A.1 (southern part). 66 β-intersections. Contours at 40-20-10-2 per cent per 1 per cent area. Dots stand for πS_1-poles.

FIG. 5. β-diagram of the bedding planes (S_1) measured within 8 metres on either side of the syncline-anticline pair, S.2–A.2. 55 β-intersections. Contours at 40-20-10-2 per cent per 1 per cent area. Dots stand for πS_1-poles.

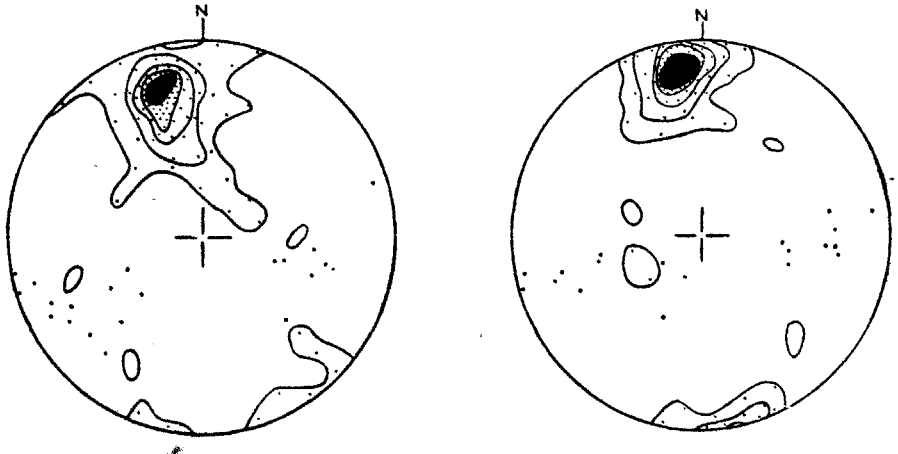

FIG. 6. β-diagram of the bedding planes (S_1) measured within 8 metres on either side of the syncline-anticline pair, S.3–A.3. 200 β-intersections. Contours at 20-15-10-5-1 per cent per 1 per cent area. Dots stand for πS_1-poles.

FIG. 7. β-diagram of the bedding planes (S_1) measured within 8 metres on either side of the syncline-anticline pair, S.5–A.5. 171 β-intersections. Contours at 20-10-5-1 per cent per 1 per cent area. Dots stand for πS_1-poles.

the axial planes of the monoclinal 'rolls' are inclined at 60°–70° eastward (Fig. 8).

By field mapping and extrapolation along strike over areas of poor or no exposures, it was possible to trace out on the map several horizons in the limestones (Fig. 9). It is of interest to note that while the traces of the horizons show V-shaped closures along the hinges of the folds, they become sub-parallel to the axial traces on the limbs of all the folds. On the west limb of the main anticline, the traces of the horizons locally trend more westerly than the NNW axial trace of the main anticline itself.

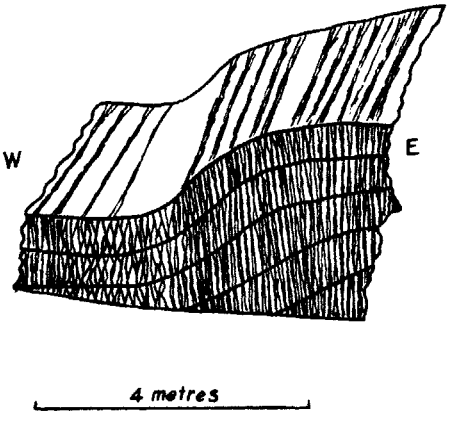

FIG. 8. Sketch of a monoclinal 'roll' on the western limb of the main anticline, A.1.

The non-divergent nature of the traces of the horizons on the limbs of the plunging folds is explained by the fact that the folds are distinctly conical on a large scale, the curvature of the folds being less towards the north than in the south. This fact is well brought out in a block diagram drawn to scale (Fig. 9). Although conical on a large scale, the folds are cylindrical in small segments.

Transverse joints.—The limestones are well-jointed. The most persistent set of joints is the one trending approximately N 80° E–S 80° W and dipping mainly to the south at steep angles (80°–90°). Being approximately perpendicular to the fold axes, this set of joints may be considered as transverse joints (Hills 1953, pp. 103-104). However, there is a distinct tendency of these joints intersecting the fold axes at an acute angle (80°–85°), as illustrated in Fig. 10*a*. Equal-area projection of the poles of transverse joints measured within 25 ft of the hinge of the main anticline also demonstrates this clearly (Fig. 10*b*).

Cleavages.—Cleavage is very well-developed in the folded limestones of the Chitorgarh Power House area. There are two categories of 'fracture cleavage' (the term is used here in the same sense as used by Leith 1905, p. 12,

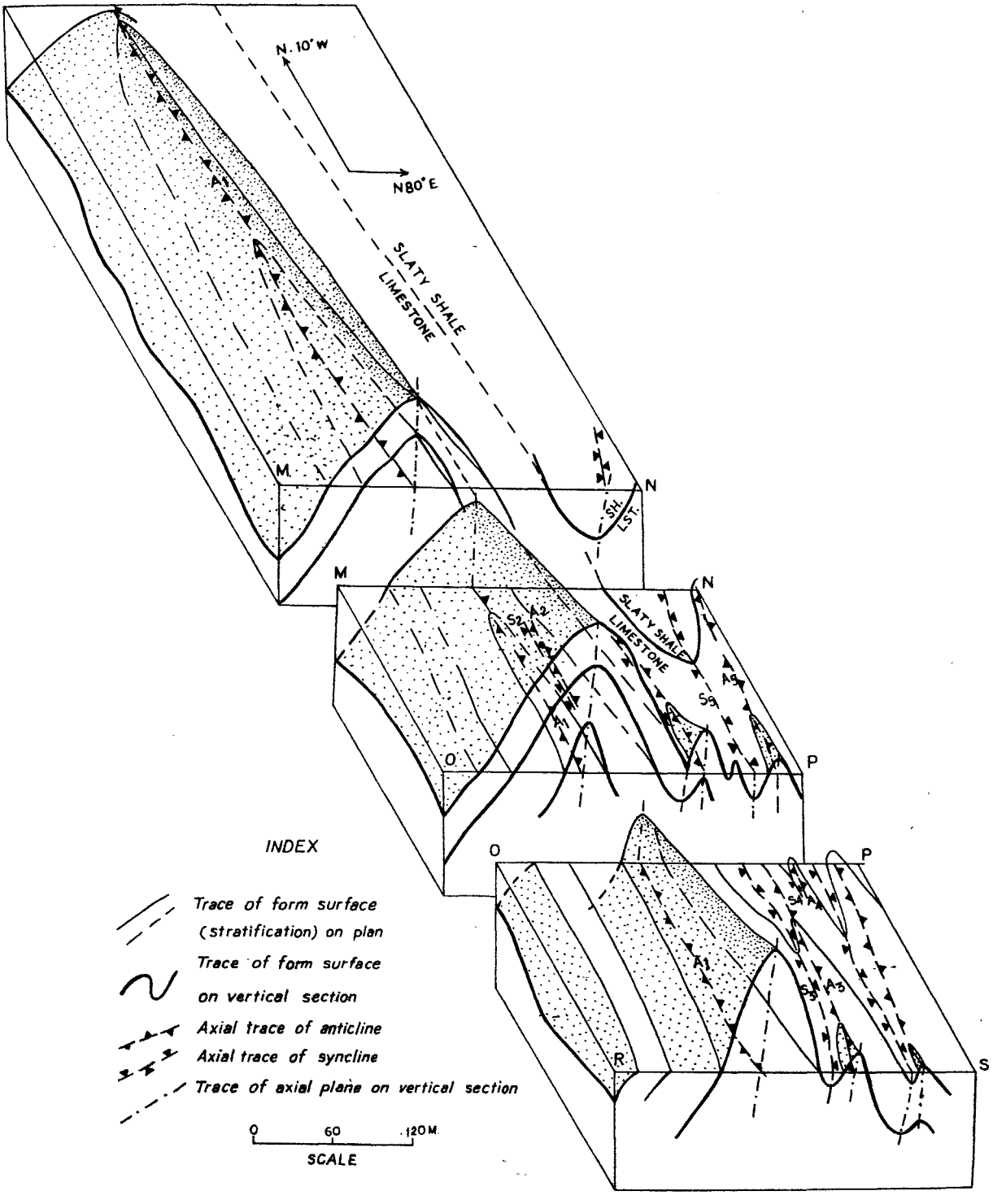

FIG. 9. Block diagram showing the folded structure of the Nimbahera limestone near Chitorgarh Power House. Locations of the sections MN, OP, RS shown on Fig. 1.

and Mead 1940, pp. 1009-1010) in these rocks: (*a*) the major cleavages (S_2, S_3) and (*b*) the minor cleavage (S_4).

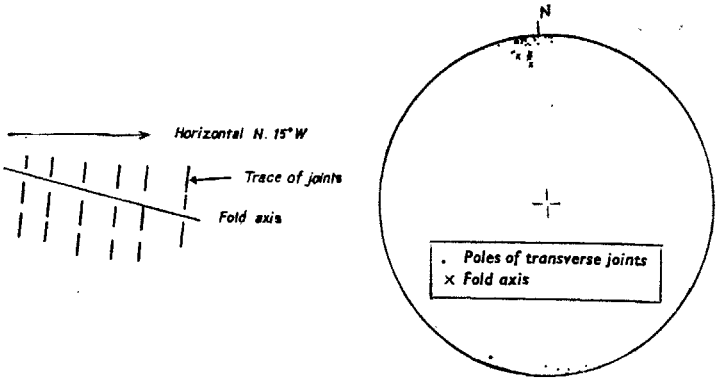

FIG. 10. (*a*) Diagram illustrating the attitude of the transverse joints in relation to the fold axes (along a section parallel to fold axis) in the Nimbahera limestones of Chitorgarh Power House area.
(*b*) Equal area projection of the poles to transverse joints measured within 8 metres of the hinge of the main anticline.

The minor cleavage (S_4) is a set of locally developed, moderately dipping (30°–64°), rather widely-spaced fracture planes (1 cm–5 cm apart); the dips on the western limb of the main anticline are towards east while those on the eastern limb are westerly (Fig. 11). The cleavage S_4 clearly cuts across the major cleavages S_2 and S_3.

The major cleavages consist of two sets of discrete, close-spaced (0·1 mm –5 mm) intersecting fracture planes (S_2, S_3), giving rise to a reticulate appearance on bedding planes and joints (Plate II, fig. 1). Careful observation of

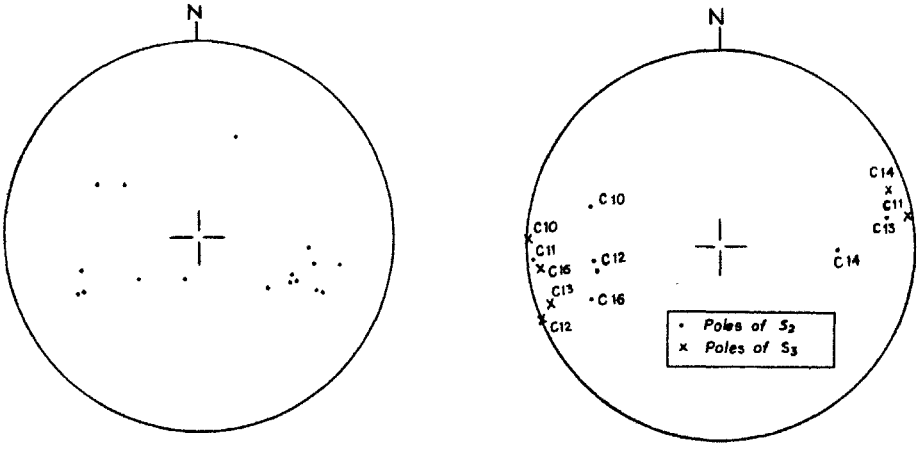

FIG. 11. Equal-area projection of the poles to fracture planes (S_4) in the Nimbahera limestone of the Chitorgarh Power House area.

FIG. 12. Equal-area projection of the poles to the fracture cleavages, S_2 and S_3, as measured in oriented specimens of the Nimbahera limestone.

hand-specimens and thin sections indicates that one of these sets (S_3) truncates the other set (S_2) and even displaces the latter through small distances (Plate II, fig. 2). In general, S_3 is steeper than S_2 (Figs. 12 and 13) and the angle between the two varies between 7° and 38°. In view of the limited time available to the authors, measurements of S_2 and S_3 were not attempted in the individual exposures in the field; it was found more convenient to measure the bisectors of S_2 and S_3, and these data are plotted in the map (Fig. 1). Remembering that at any spot $S_2 \wedge S_3$ is about 20° on an average and that S_3 is always steeper than S_2, the bisector data (Fig. 1) are useful in understanding the attitude of the cleavages throughout the area.

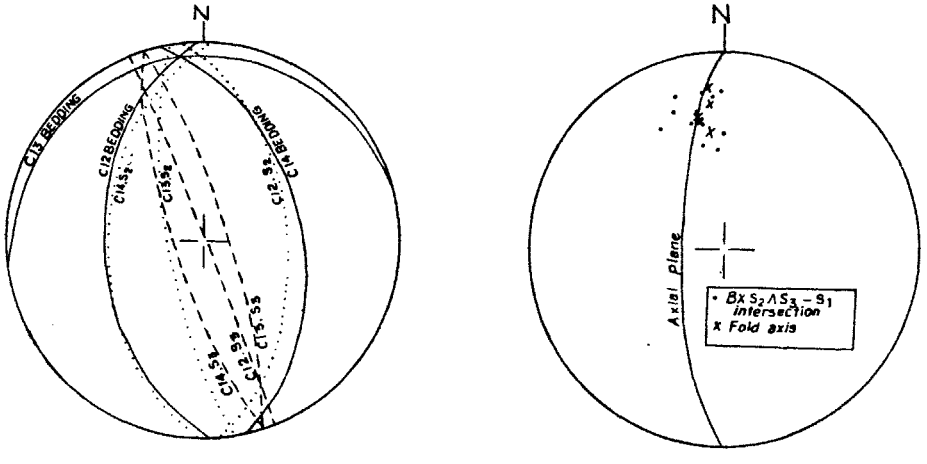

FIG. 13. Equal-area projection of the bedding and fracture cleavages, S_2 and S_3, as measured in three oriented specimens of the Nimbahera limestone collected across the anticline, A.5.

FIG. 14. Equal-area projection of the data on measured fold axes and the $BXS_2 \wedge S_3 - S_1$ intersections within 3 metres of the hinges anticline-syncline pair, A.3–S.3.

Geometric relationships between major cleavages and bedding.—The major cleavages (S_2 and S_3) are related to the bedding (S_1) of the limestones in the following ways:

1. The cleavages occur on the limbs as well as on the hinges of the folds, but are slightly more prominent on the hinges.

2. On any limb of a fold, both S_2 and S_3 intersect the bedding (S_1) at high angles and generally dip in a direction opposite to that of the bedding. However, the cleavage-bedding angle on the hinges (nearly 90°) is always higher than that on the limbs.

3. Both S_2 and S_3 show clear fanning with respect to the folds with downward convergence in the anticlines and upward convergence in the synclines. Fanning of S_2 is, however, greater than that of S_3, as illustrated by the stereoprojections of the cleavages and bedding in three oriented samples collected across the anticline, A.5 (Fig. 13).

4. The S_2–S_1, S_3–S_1 as well as the S_1–$BXS_2 \wedge S_3$ intersections at locations within about 8 m of the hinges of the folds lie close to the fold axes as measured directly or by bedding plane intersections (Figs. 13 and 14). However, there is always a small but significant divergence (maximum 26°) between the cleavage-bedding intersections (viz. S_2–S_1, S_3–S_1 and $BXS_2 \wedge S_3$–S_1) and the corresponding fold axes. The S_2–S_3 intersections seem to lie even farther from the corresponding fold axes, viz. up to 38° (Fig. 13).

5. The angles between the fold axis and the cleavage-bedding or cleavage-cleavage intersections are greater on the limbs than near the hinges. The maximum angle recorded for the F.A. $\wedge$ (S_1–$BXS_2 \wedge S_3$ intersection) is 43° and that for the F.A. $\wedge$ (S_2–S_3 intersection) is 45° as calculated from data in Table II.

6. The angles $S_2 \wedge S_3$ tend to be the least on the hinges of folds (Table II).

7. The Suket slaty shales overlying the limestones near the Power House show a prominent cleavage which intersects the lamination generally at high angles. The cleavage-bedding relationship here is similar to that in the limestone, but it is not clear whether the prominent fracture cleavage in the slaty shales corresponds to S_2 or to S_3 of the limestone.

Displacement along the cleavage planes.—Minute displacements of the laminations in limestone along both S_2 and S_3 are characteristic, displacements along the latter being more prominent (Plate II, figs. 3 and 4). Normally such displacements are less than 1 mm, but near the hinges of the folds slip on S_3 may be up to 5 mm.

Microscopic study indicates that within the finely crystalline granular aggregate of calcite, S_3 occurs as a set of very close-spaced, clear-cut planes, usually coated with brownish stains. S_2, on the other hand, is a set of relatively wide-spaced fracture planes, filled with comparatively coarse crystals of calcite which in places are elongated (0·1–0·5 mm long), the elongation being mostly parallel to the S_3 planes in the rock; S_3 fractures traverse through the calcite-filled S_2 fractures (Plate II, fig. 2). Aggregates of elongated calcite crystals occur also in local bands along S_1. Locally the elongation of calcite crystals along S_2 tends to be parallel to the S_2 fracture, but even there such crystals are visibly bent in a manner suggesting that these have been forced to align themselves parallel to S_3.

The manner of slip of bedding on S_3 deserves scrutiny. Near the anticlinal hinges the bedding (S_1) is displaced *en bloc* (cf. Plate II, figs. 3 and 4) in a pattern suggesting relative upward displacement towards the crest of an anticline, and these S_3 cleavage planes might be described as small-scale faults (cf. Badgley 1959, Fig. 38). The direction of slip along S_2 seems to be rather irregular.

The average attitudes of the elongation axis of the elongated calcite crystals lying parallel to the S_3 planes were measured in several oriented thin sections of the limestone.

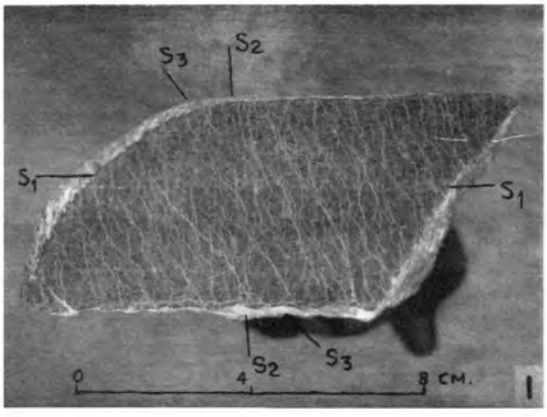

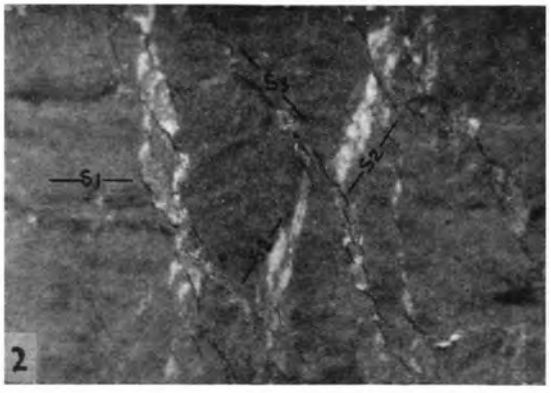

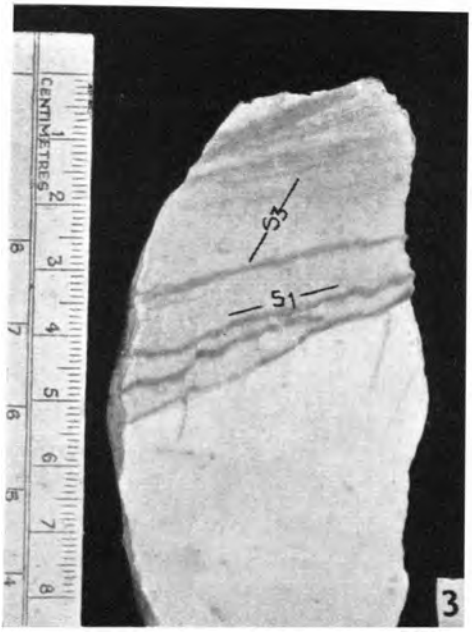

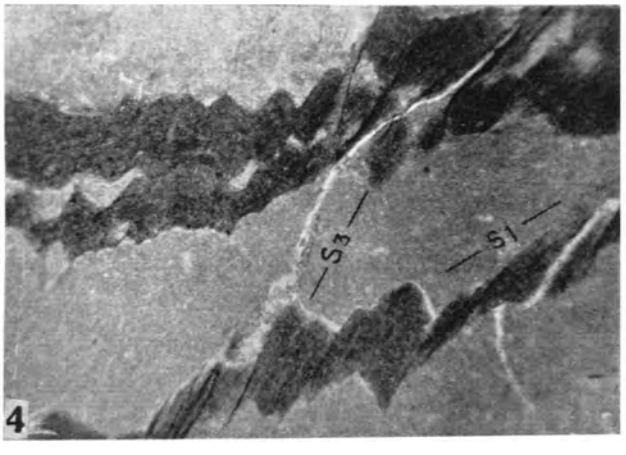

FIG. 1. Photograph of a specimen of the Nimbahera limestone of the area showing two sets of fracture cleavages, S_2 and S_3, and bedding, S_1.

FIG. 2. Photomicrograph prepared from the specimen in Plate II, fig. 1, showing displacement of S_2 by S_3; calcite crystals along S_3 are partly bent to a parallelism with S_3. Parallel light. × 30.

FIG. 3. Photograph of a hand-specimen of the Nimbahera limestone illustrating the displacement of bedding (S_1) by fracture cleavage (S_3).

FIG. 4. Photomicrograph prepared from the specimen in Plate II, fig. 3, showing irregular *en bloc* displacement of bedding (dark grey layers) by S_3. Parallel light. × 20.

The axis of elongation as measured on each thin section was transferred on the S_3 plane by rotating its pole stereographically along the plane normal to the plane of section and passing through the trace of the elongation on the plane of section. The data obtained in this way (Table II) are suggestive of sub-vertical movements along S_3.

It should be emphasized here that the elongated calcite crystals occupy only a very small bulk of the limestone, the greater part of which consists of a finely crystalline, equigranular aggregate.

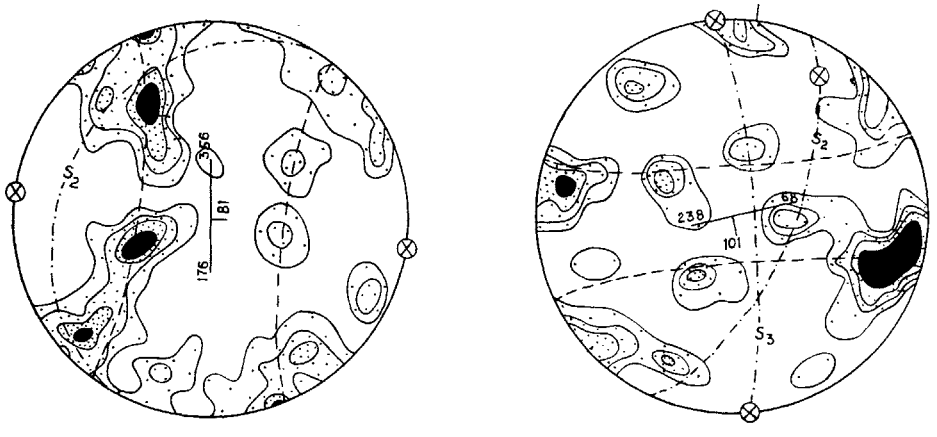

FIG. 15. Orientation diagram of 200 optic axes of elongated calcite grains in a specimen (C.16) of limestone; contours at 4-3-2-1 per cent per 1 per cent area (maximum 5·5 per cent). Plane of projection is parallel to S_3; circled cross represents the average axis of elongation of the crystals. Dashed lines give the trace of the 60° small circle around this axis.

FIG. 16. Orientation diagram of 128 optic axes of elongated calcite grains in a specimen (C.14) of limestone; contours at 5-3-2-1 per cent per 1 per cent area (maximum 6 per cent). Circled crosses represent the average axes of elongation of crystals sub-parallel to S_2 and S_3 respectively. Dashed lines give the trace of the 70° small circle around the axis of elongation parallel to S_3.

Orientation patterns of the calcite optic axes.—A statistical study of the *c*-axis orientation of the moderately coarse elongated calcite crystals in two oriented specimens (C.16 and C.14) of the limestone was carried out. The attitudes of the S planes in these two specimens are given in Table II. In both, the elongated crystals are sub-parallel with the S_3 planes and show distinct preferred orientation. In C.16, where S_3 is very well-developed but S_2 is ill-developed, a well-defined small-circle, cleft girdle of *c*-axis at 60° from the average axis of elongation of the crystals is clearly recognizable (Fig. 15); internal concentrations in the girdle suggest triclinic symmetry. In the other specimen (C.14), where a prominent S_2 lies at a high angle with an equally prominent S_3, the *c*-axis pattern is triclinic and rather unsystematic (Fig. 16). However, here too, a small-circle cleft girdle at about 70° from the average elongation axis of most of the elongated crystals is recognized.

TABLE II

Attitudes of the structures in several oriented specimens of Nimbahera limestone, Chitorgarh

Specimen number	S_1	S_2	S_3	$S_1 \wedge S_2$	$S_1 \wedge S_3$	$S_2 \wedge S_3$	Calcite elongation	Location of specimen
C.10	46°/N 58° W	58°/S 72° E	88°/S 86° E	75°	50°	34°	62°/S 2° E	44 m west of A.1
C.11	6°/N 8° W	84°/N 88° E	87°/S 84° W	88°	86°	7°	64°/S 2° W	Hinge A.1
C.16	45°/N 80° W	60°/N 70° E	81°/N 86° E	78°	52°	26°	78°/S 55° W	26 m west of A.1
C.12	48°/W	55°/N 86° E	89°/N 70° E	76°	45°	38°	65°/N 15° W	60 cm west of A.5
C.13	8°/N 7° W	75°/S 82° W	80°/N 74° E	76°	81°	24°	Not clear	Hinge A.5
C.14	49°/N 78° E	50°/N 86° W	78°/S 74° W	82°	53°	34°	76°/N 55° W	1·5 m east of A.5

In this specimen some of the elongated crystals are sub-parallel with S_2 and many of these are visibly bent to a parallelism with S_3. A rudimentary, small-circle girdle at 30°–40° from the average axis of elongation of the crystals sub-parallel to S_2 is discernible.

Other structures.—Among the other structures of the limestone in the Power House area the local zones of 'drag' on the eastern limbs of the main anticline are of special interest. Along these zones (barely 2 m × 1 m) the steep dipping limestones are drag-folded about steep dipping, NW–SE trending axial planes with considerable shearing along these zones. Extensive veins and pockets of white calcite crystals characterize these zones. Locally the hinges of the folds A.3–S.4 are also affected by such drag.

3. Interpretation of the Structures

A. Nature of the folding.—As already noted, the folds are cylindroid on a small scale and slightly conical on a large scale. Also the fact that the thicknesses measured perpendicular to bedding on the hinges and the adjacent

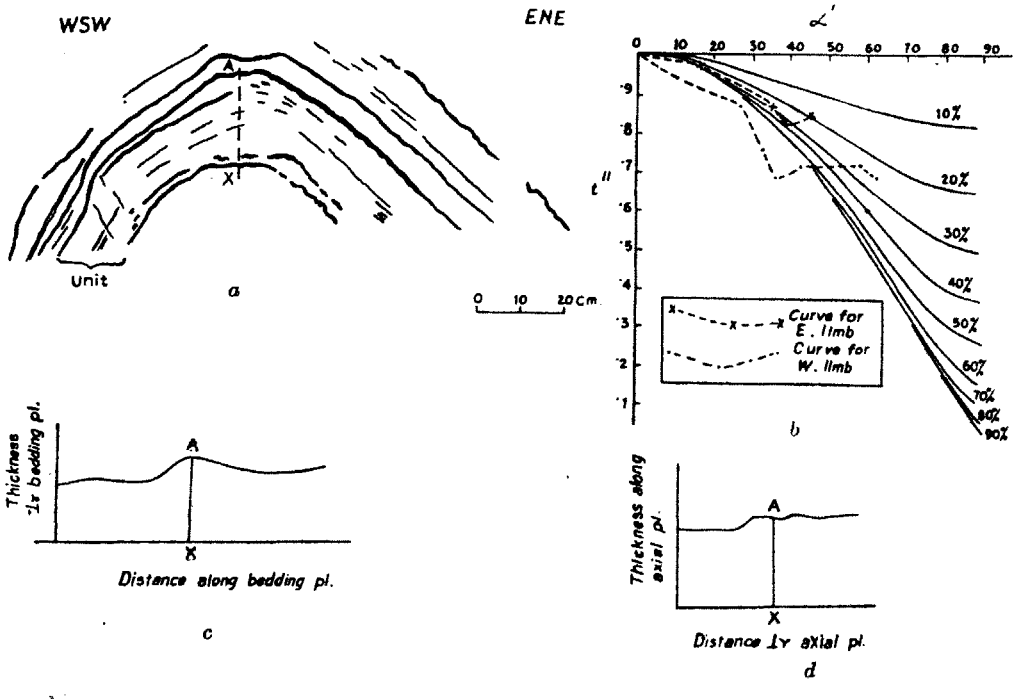

Fig. 17. (*a*) Profile No. 1 of the anticline A.2, cleavage details omitted.
(*b*) Graph showing α′ (bedding dip) in relation to *t*″ (thickness of a bed where bedding dips at α′/thickness at fold hinge). Solid curves give amounts of flattening (after Ramsay 1962, Fig. 7).
(*c*) Graph showing thickness normal to bedding against distance along bedding plane.
(*d*) Graph showing thickness parallel to axial plane against distance normal to axial plane.

limbs are in general uniform, suggests that the folds are mainly concentric in nature. There being no evidence of the effect of relative tension and compression in the upper and lower layers of a bed, pure bending as the mechanism of folding is not favoured here (Billings 1954, p. 89). The folds thus appear to have been produced by flexural slip of the successive layers of the limestone. In this connection notable thickening of the crests and troughs as observed in some of the folds needs explanation. The profile of an anticline A.2 has therefore been studied quantitatively at two places (Figs. 17 and 18). Following Ramsay (1962), the values of α' (bedding dip) and t'' (thickness of a bed where bedding dips at α'/thickness at fold hinge) were measured at a number of spots on both the limbs of the anticlines and the results plotted graphically. The patterns for both the profiles suggest no uniform flattening (Ramsay 1962) of the rocks, but slips of unequal magnitude at discrete intervals. Displacements of the thin beds along the cleavages (particularly along S_3) do suggest the influence of slips in determining the shapes of the folds. Other interesting results of the measurements of the two profiles are that (i) in both the cases the limestone beds measured show an original slight thickening eastward (Figs. 17 and 18) and (ii) the thicknesses measured parallel to the axial plane also show small but irregular variations, such variations being attributable to irregular slips.

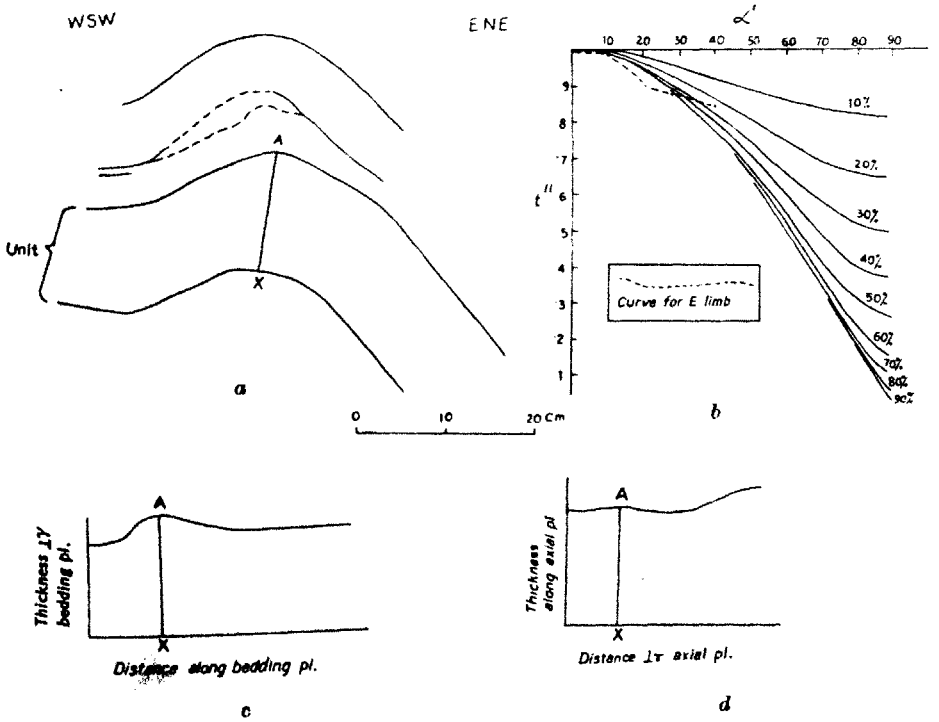

FIG. 18. (*a*) Profile No. 2 of the anticline A.2, cleavage details omitted. (*b*), (*c*), (*d*) as in Fig. 17.

It appears, therefore, that the folds in the present area are concentric folds, the shapes of which have been modified, at least in places, by the effects of irregular slips along the cleavages, especially S_3.

B. The major cleavages.—The following important aspects of the major cleavages need rational explanation: (*a*) the fact that the cleavage-bedding intersections show small but significant deviations from the axes of the folds, (*b*) fanning of the cleavages with respect to the folds, (*c*) the relationship between S_2 and S_3 and (*d*) the mechanism of formation of the cleavages.

As regards the relationship between S_2 and S_3, several alternative possibilities may be considered as follows:

(i) they are conjugate shear planes that developed before folding;

(ii) they are conjugate shear planes that developed concomitantly with the flexural slip folding;

(iii) they are conjugate shear planes that developed after the folding;

(iv) they are *not* conjugate shear planes; S_2 developed in the earlier stages, and S_3 in the later stages of the folding, either (*a*) approximately parallel to the prevailing attitude of the axial planes of the folds (i.e. along the AB plane of the strain ellipsoid), or (*b*) by oblique shear, at an angle with the prevailing axial planes (cf. De Sitter 1956, p. 99).

Let us consider now the arguments *for* and *against* each of these alternatives:

(i) If S_2 and S_3 had developed before the folding, we would expect nearly constant angle between the bedding and the respective cleavages.

Actually, the bedding-cleavage angles are consistently greater on the hinges than on the limbs. Further, the distribution of S_2 and S_3 throughout the area in a fanned arrangement around all the nine folds strongly suggests genetic connection between the folds and the cleavages S_2, S_3.

(ii) If both S_2 and S_3 were developed as conjugate shear planes during the folding, we should expect both to show the same degree of fanning; also displacement of S_3 by S_2 should be found along with displacement of S_2 by S_3. Actually S_2 is clearly more fanned than S_3 and S_3 is never displaced by S_2.

(iii) S_2 and S_3 could not possibly have developed as conjugate shear planes after the fold movements because, in that case, the lower $S_2 \wedge S_3$ on the hinges of folds than on the limbs cannot be explained.

(iv) S_2 and S_3 cannot therefore be regarded as conjugate shear planes, whether developed before, during or after the fold movements. We are thus left with the hypothesis that S_2 developed earlier than S_3—both during the fold movements. The facts that (*a*) S_2 shows greater fanning around the folds than S_3 and (*b*) S_3 always displaces S_2 support this. We may picture the S_2 cleavage as having developed at an early stage of folding; their concomitant rotation during concentric folding accounts for their pronounced fanning; the S_3 planes seem to have developed at a late stage of

folding but well before the close of the fold movements, because fanning of S_3 is also prominent (Fig. 19). On the other hand, the clear-cut nature of the S_3 fractures and the pronounced displacements of S_1 and S_2 along them might suggest that the movements along S_2 may have continued even after the end of the fold movements.

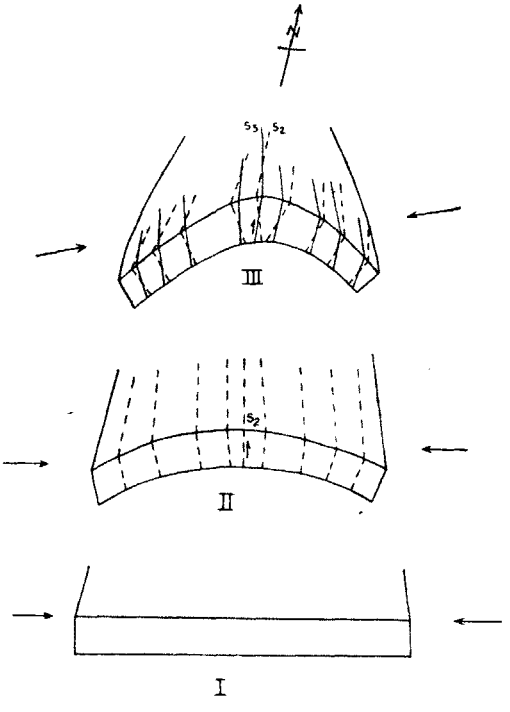

FIG. 19. Diagrammatic representation of three stages of folding and development of S_2 and S_3 in the Nimbahera limestones near Chitorgarh Power House. Arrows indicate the approximate attitudes of the maximum stress axis.

The sub-parallelism of both S_2 and S_3 with the present attitude of the axial planes of the folds, especially at and near the hinges, suggests that the cleavages were initiated along the AB plane of the strain ellipsoid (Hills 1953, pp. 105-106; De Sitter 1956, pp. 214-215; Williams 1961). Alternatively, they could represent planes of oblique shear (cf. De Sitter 1956, pp. 98-99), the shear planes being rotated to a sub-parallelism with the axial planes of the folds as a result of bedding plane slip. However, bedding plane slip would be effective only on the limbs and *not* on the hinges; it is remarkable that the fracture cleavages are sub-parallel to the axial plane even on the hinges—in fact, such parallelism is more marked on the hinges than on the limbs. The fact that both the fracture cleavages, S_2 and S_3, are more prominent on

the hinges than on the limbs of the folds rules out the possibility of their development by bedding plane slip (cf. Wilson 1946).

An important problem that arises in this connection is how to explain the small but distinct deviations of the S_2–S_1, S_3–S_1 and S_1–$BXS_2 \wedge S_2$ intersections from the observed fold axes, even for data near the hinges of the folds. In the light of available data, the most probable explanation of this is as follows:

The attitudes of the strain ellipsoid in the limestones varied within certain limits during the fold movements. Thus, although the S_2 fractures originated parallel to the axial plane of the folds, the attitude of the axial planes may have changed with the progress of folding, giving rise to the non-parallelism of the S_2–S_1 intersections with the present attitude of the fold axes. The same explanation should apply in the case of S_3.

There is, in fact, some evidence in favour of the idea of the variations in the strain pattern during the period of folding as follows:

(*a*) As will be evident from Table I and Fig. 13, the S_3 planes have relatively more westerly strikes than the corresponding S_2; this might mean that during the formation of S_3 the attitude of the sub-horizontal least strain axis was nearly ENE-WSW, while that during the formation of S_2 was nearly east-west.

(*b*) The poles of transverse joints (Fig. 10*b*) plunge at a much lower angle than the fold axes. Since these apparently developed at a late stage of folding, it might be suggested that the B axis of the strain ellipsoid was nearer horizontal during the late stages of folding than in the earlier stages.

(*c*) The cleft-girdle pattern of *c*-axis with maxima in a small circle at 60°–70° with the direction of grain elongation, as found in both the oriented specimens studied, is common in calcite tectonites with markedly elongated grains. The girdle axis in such cases indicates the axis of the minimal principal stress, σ_3 (Turner and Weiss 1963, p. 413). Also experimental studies by subjecting marble cylinders to non-rotational stress indicate that the maxima of *c*-axis tend to be located at 20°–30° with the σ_1-axis (Turner and Weiss 1963, pp. 348–351). From these known data on the calcite *c*-axis fabric, it would appear that the main girdle axes in the two specimens give the attitudes of the minimal principal stress axis σ_3 during the movements on S_3. The attitudes of σ_3, as deduced from the diagrams, are 78°→S 55° E and 76°→N 55° W (rakes on S_3 being 82° S and 80° N respectively).

The σ_1-axis cannot, however, be located from these diagrams. The triclinic symmetry of both the diagrams (Figs. 15 and 16) probably reflects the orienting influences of a changing pattern of the stress axes.

The average elongation axis of the crystals parallel to S_3 as measured in three other oriented specimens also have sub-vertical dispositions (Table II), as in the specimens C.16 and C.14. Presumably, the attitudes of the minimal

principal stress axis σ_3 (during the movements along S_3) is sub-vertical in these specimens too. The petrofabric data thus suggest strongly that the pronounced slip on S_3 was accompanied by extension of the rocks in a sub-vertical direction.

C. The minor cleavages.—From the observed cross-cutting relationships, S_4 is clearly later than S_2 and S_3. The S_4 planes dip westward on the eastern limb and eastward on the western limb of the main anticline, but seem to be unaffected by the subsidiary folds on the eastern limb of the main anticline. This observation suggests that S_4 may have developed at a late stage of the fold movements when the fold movements along the subsidiary folds ceased. The distinct attitudes of the S_4 planes on either limb of the main anticline (Fig. 11) suggest that we are dealing here with two sets of conjugate fractures nearly normal to each other, one of the bisectrices being approximately sub-horizontal and east-west. Formation of the zones of 'drag' was also clearly later than the development of the subsidiary folds on the eastern limb of the main anticline, but whether they are synchronous with S_4 or not cannot be decided with the data at hand.

4. The Sequence of Events

The formation of the folds and the cleavages in the Nimbahera limestones of Chitorgarh Power House area is thus interpreted as responses of the rock to a single episode of deformation, and there is a genetic, but not necessarily a cause-and-effect relation, between these processes. The history of deformation is summarized as follows:

1. The Nimbahera limestone was folded on NNW axes by flexural slip. A set of fracture cleavages, S_2 (parallel to the axial plane of the folds), developed at an initial stage of folding and helped in the extension of the rock mass by minor slip.

2. With continuation of folding, S_2 became passive and another set of fracture cleavages, S_3, developed along planes parallel to the prevailing axial planes of the folds; pronounced slip on S_3 helped extension in a sub-vertical direction. Attitude of the sub-horizontal least strain axis appears to have varied within certain limits during the progress of folding—this being nearly east-west at the time of initiation of S_2 and nearly ENE-WSW at the time of formation of S_3.

3. During the waning stage of deformation a set of transverse joints, a set of minor, rather wide-spaced cleavages (S_4) and certain zones of 'drag' developed.

Acknowledgements

The authors are grateful to Professor S. Ray, Head of the Department of Geology, Presidency College, Calcutta, for providing facilities for the field

and laboratory studies represented in this paper. Their thanks are due to Dr. S. Deb, F.N.I., Jadavpur University, for kindly going through the manuscript.

References

Badgley, P. C. (1959). Structural Methods for the Exploration Geologist. Harper & Bros., N.Y., pp. 1–280.

Billings, M. P. (1954). Structural Geology. Prentice-Hall, N.Y., pp. 1–514.

De Sitter, L. U. (1956). Structural Geology. McGraw Hill, N.Y., pp. 1–552.

Heron, A. M. (1936). The geology of South-eastern Mewar, Rajputana. *Mem. geol. Surv. India*, **68**, pt. 1, plate 22.

Hills, E. S. (1953). Outline of Structural Geology. Methuen, Long., pp. 1–182.

Leith, C. K. (1905). Rock Cleavage. *Bull. U.S. geol. Surv.*, 239.

Mead, W. J. (1940). Folding, rock flowage, and foliate structures. *J. Geol.*, **48**, 1007–1021.

Ramsay, J. G. (1962). The geometry and mechanism of formation of 'similar' type folds. *J. Geol.*, **70**, 309–327.

Turner, F. J., and Weiss, L. E. (1963). Structural analysis of metamorphic tectonites. McGraw Hill, N.Y., pp. 1–545.

Wilson, G. (1946). The relationship of slaty cleavage and kindred structures in tectonics. *Proc. Geol. Asso.*, **57**, 263–302.

Williams, E. (1961). The deformation of confined, incompetent layers in folding. *Geol. Mag.*, **98**, 317–323.